EISEVIED

Contents lists available at ScienceDirect

# **Powder Technology**





# Influence of guest and host particle sizes on dry coating effectiveness: When not to use high mixing intensity



Kai Zheng, Kuriakose Kunnath, Zhipeng Ling, Liang Chen <sup>1</sup>, Rajesh N. Davé \*

New Jersey Center for Engineered Particulates, New Jersey Institute of Technology, Newark, NJ 07102, USA

#### ARTICLE INFO

Article history: Received 21 November 2019 Received in revised form 19 February 2020 Accepted 22 February 2020 Available online 24 February 2020

Keywords:
Dry coating
Process intensity
Guest particles
Host particles
Dry coating quality
Stick/bounce model

#### ABSTRACT

The effects of material stiffness, host and guest particle sizes, and mixing intensity on dry coating quality were investigated using a high-intensity vibrational mixer, using KCl, cornstarch, aluminum silicate and nano-sized silica. The coating quality deteriorated with larger guest particle size at high process intensity, and high material stiffness. Coarse guest particles detached from host particles above certain mixing intensity, indicating higher intensity is not recommended; e.g., the best coating quality for cornstarch was for medium-sized hosts below 30 Gs intensity. However, for nano-silica guests, higher processing intensity did not lead to their detachment, but decreased their agglomeration. Such behavior was explained using the energy-based stick/bounce model and two indices. The coating quality index ( $K_c$ ), the ratio of total detachment energy to relative kinetic energy, assessed the guest particle attachment tendency. The deagglomeration index ( $K_d$ ), the ratio of deagglomeration energy to relative kinetic energy, assessed the guest particle agglomeration tendency.

© 2020 Elsevier B.V. All rights reserved.

#### 1. Introduction

Dry particle coating is an innovative process to alter the surface properties and/or functionality of particles by placing smaller guest particles on larger host particle surfaces [10,39,40,47,53,54]. In the process of dry coating, the guest particles stick or get embedded on the surface of the host particles as has been shown in excellent previous papers on ordered mixtures [2,23]. The guest particles get attached to the host particles primarily due to their van der Waals attraction, as initially chunks of agglomerated guest particles attach on to the host particle surfaces. Then, repeated collisions of the host particles lead to transfer/dispersion of the guest particles and eventual surface coating [14,47,53]. Since it does not use solvents during processing, it could be used for diverse materials and applications to prepare coated particles. Published examples of its use include; improvement in powder flow after coating with very small amounts of nano-silica [12,18,30,40,47,53,54], improvement in packed bed porosity [8], enhanced fluidization of fine particles [12], coating with a polymer film [13], deactivation of sintering after dry coating glass beads with sub-micron silicon carbide [17,49], increased humidity resistance of fine ground magnesium powders [36], enhanced dissolution of tablets that includes hydrophilic silica coated ibuprofen [20], improved combustion of aluminum powders after coating with carbon black [31] and even an intriguing example where boron nitride powders coated with nano iron oxide facilitated in-situ growth of carbon nanotubes [44]. Examples from pharmaceutical applications include improving content uniformity of blends and powder flow, engineered excipients, and even achieving film coating leading to controlled release of drug products [6,7,10,12,22,27,34,53].

The comparative study of Yang [53] and subsequent reports suggest that dry coating requires high-intensity mixing devices, such as the mechanofusion, the hybridizer [24,39,40,47,54], magnetically assisted impaction coating (MAIC) [18,30,47,53] and recently developed devices such as the fluid energy mill (FEM) [19,21,55], the conical screen mill [25,38], and a high-intensity vibration device called the LabRAM [26]. In addition to using high-intensity devices, most of the literature has only considered use of nano or sub-micron sized guest particles, and generally concluded that the host particles need to be one or two orders of magnitude larger. However, considering its potential for more diverse applications including using larger guest particles, there is a need to develop better understanding of the factors such as the guest and host particle sizes, their material properties, the processing devices, and their operating conditions that enable better coating. Towards that goal, previous work included phenomenological explanation [3,47] and modeling efforts such as estimating process time through analysis of collision frequency and energy, assuming the velocity distribution for the fluidized state to be Maxwell-Boltzmann [50], or examining the device level dynamics using the discrete element method (DEM) modeling [11,14,15], or using highly simplified, reduced order device models [4]. There have also been advances in the understanding of resulting particle behaviors after dry powder coating based on the interactions between particles accounting for their surface roughness, surface

<sup>\*</sup> Corresponding author.

E-mail address: dave@njit.edu (R.N. Davé).

<sup>&</sup>lt;sup>1</sup>Current address: Product and Technical Development, Biogen, 225 Binney St., Cambridge, MA 02142. United States

energy and particle sizes [9,12,35,53]. For example, the *Chen* model [12] extended the *Rumpf* model to account for multi-asperity contacts, so that the interparticle adhesion force before and after dry coating could be estimated, while accounting for the extent of guest particle coverage of the host particle surface. Unfortunately, the effects of particle properties such as their sizes, stiffness and surface energies on the coating effectiveness have not been investigated while simultaneously accounting for the mixing intensity; which is the topic of the present work. For the purpose of such investigation, the coating effectiveness may depends on the total number of guest particles that stick on the host particle surface, quantitatively defined by the extent of the host particle surface covered by the guest particles, see for example image analysis based evaluation in a previous study [53].

Particle properties, mixing time and intensity can exert a great influence on the performance of dry powder coating processes [14,26,27,42,53]. Higher mixing intensity is recommended to facilitate uniform dispersion of guest particles and reducing mixing time [14,26,33,37,53]. Unfortunately, higher mixing intensity has disadvantages such as higher energy cost, risk of particle attrition, and increased processing temperatures requiring special cooling [7,14,27,30,47]. To date however, the selection of process intensity, while simultaneously accounting for the properties of both guest and host particles, in particular for the guest particles that are not nano-sized, remains underinvestigated. Such knowhow would enable design of a wider variety of materials where the guest particle need not be or cannot be nanosized; e.g., such as wax particles, polymeric beads, magnesium stearate, or micro-sized active ingredients [6,7]. Towards that goal, the stick/ bounce approach of Thornton and Ning where either the relative momentum, or the relative kinetic energy and van der Waals (vdW) energy change during particle collisions, could be used for estimating the stick/ bounce state after collisions [1,51]. Here, the energy-based approach will be considered.

In what follows, the particle material properties, effects of particle sizes, and mixing intensity are investigated to understand the mechanism of the dry powder coating process and performance. First, theoretical aspects of particle interactions and the energybased stick-bounce approach are presented so that the particle adhesion energy, relative kinetic energy of collisions, plastic deformation energy, and the deagglomeration energy can be computed to analyze the detachment and deagglomeration of guest particles. These computations consider the host and guest particle sizes and their material properties derived from available literature. For the experimental investigation, the commercially available highintensity vibrational mixer, called the LabRAM, is considered. Additionally, the host and guest materials as well as the characterization methods used in this study are described. The results of the effects of material stiffness and the guest and host particle sizes along with the process intensity are presented. Finally, the quality index of dry coating  $(K_c)$  for assessing the performance of dry coating, and the deagglomeration index  $(K_d)$ , which assesses the guest particle agglomeration tendency are introduced. The results of this work are expected to help better understand the dry coating process.

# 2. Theoretical

Previous studies suggest that the energy-based or momentum-based stick/bounce models may provide similar sticking/bouncing trends after collision [1]. Here, the energy-based stick/bounce model was used. According to the model, when two particles collide, the initial relative kinetic energy of particles reduces to zero and is stored as elastic energy. Subsequently, the stored elastic energy converts into relative kinetic energy again and the particles move in the opposite directions with a final kinetic energy. During the dry coating process, some energy is dissipated due to particle-plastic deformation. In addition, some kinetic energy is consumed in the deagglomeration process [14], and needs to be accounted for in the

model as well. Thus, final relative kinetic energy is always less than initial relative kinetic energy. If the final relative kinetic energy is large enough to overcome the total detachment energy (vdW energy, plastic deformation energy and deagglomeration energy) between particles, the guest particle will bounce off of the host particle. Otherwise, the guest and host particles will stick together [1]. There are several sources of losses, for example, some energy is dissipated in both the coating and de-agglomeration processes, whereas some of the kinetic energy is transferred to heat. Therefore, it is necessary to account for the energy loss in the model. Here, it is assumed that the dissipated energy is consumed in the particle deformation process. In addition, since de-agglomeration is necessary for coating, it is necessary to include the energy to overcome agglomerations in the total detachment energy. In the following, all the necessary terms are discussed and to further help evaluate the results, a quality index of dry coating  $(K_c)$  is defined. It is the ratio between relative kinetic energy and sum of vdW energy, plastic deformation energy and deagglomeration energy. All the particulate materials investigated are assumed as idealized plastic materials in form of uniform size spheres having smooth surfaces.

# 2.1. van der Waals energy

In order to understand the dry powder coating process, the interactions between particles, such as  $van\ der\ Waals\ (vdW)$ , electrostatic, and capillary forces need to be considered [29]. In dry powder coating, vdW forces are considered to be the dominant inter-particle ones, as compared to weaker electrostatic and capillary forces [9]. Hence only vdW forces are considered. As depicted in Fig. 1, the guest (fine) and host (coarse) particles deform during the collision. According to  $Israelachvili\ [29]$ , the vdW energy ( $Israelachvili\ [29]$ ) between macroscopic spheres can be estimated as the sum of contact energies between their deformed surfaces in direct contact and between rest of the surfaces not in direct contact:

i)  $E_{vdW}$  between two deformed surfaces  $(E_d)$ , which is given by:

$$E_d = \frac{HS}{12\pi\delta^2} \tag{1}$$

where H is the Hamaker constant, S is the contact area between two flat surfaces (Eq. (3)), and  $\delta$  is atomic scale separation distance, for which a value of 0.165 nm is normally used.

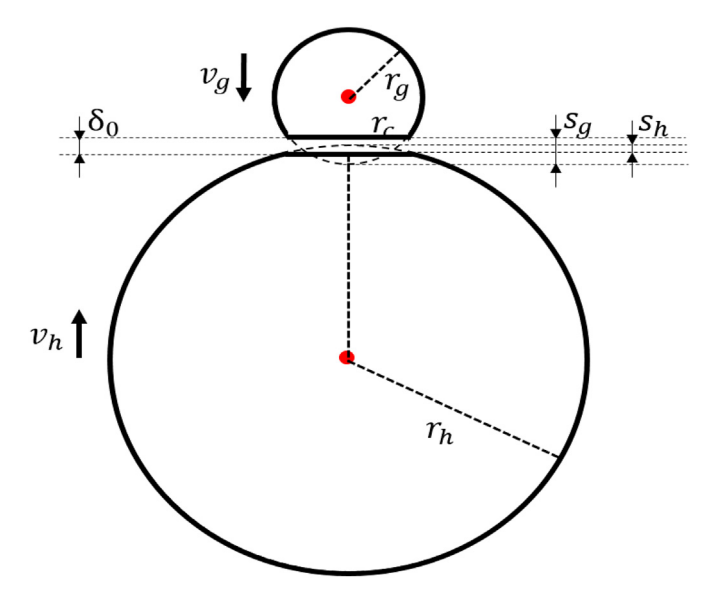


Fig. 1. Schematic of the deformed particles in contact.

ii)  $E_{vdW}$  between the rest of the surfaces of two spheres  $(E_s)$  is given by:

$$E_{\rm S} = \frac{H}{6\delta} \frac{r_h r_g}{r_h + r_g} \tag{2}$$

where  $r_h$  and  $r_g$  are the radii of host and guest particles respectively. According to Fig. 1, the contact surface area of two deformed particles can be calculated as:

$$S = \pi r_c^2 \tag{3}$$

where  $r_c$  is contact radius. According to *Hertzian* contact model [32],  $r_c$  can be given by:

$$r_{c} = \left(\frac{3F\left(\frac{1-\nu_{h}^{2}}{E_{h}} + \frac{1-\nu_{g}^{2}}{E_{g}}\right)}{4\left(\frac{1}{r_{h}} + \frac{1}{r_{g}}\right)}\right)^{\frac{1}{3}}$$
(4)

where  $\nu_h$  and  $\nu_g$  are *Poisson*'s ratios of host and guest particles respectively, and  $E_h$  and  $E_g$  are *Young*'s moduli of host and guest particles respectively. F is the contact force between fine and coarse particles, which can be estimated as:

$$F = \frac{\hat{m}\Delta v}{t} \tag{5}$$

where  $\hat{m}$  is the relative mass (given in Eq. (10)),  $\Delta v$  is the relative velocity change before and after collision, and t is the collision time, which is estimated as [45]:

$$t = 2.86 \left( \frac{\hat{m}^2 \left( \frac{1 - \nu_h^2}{E_h} + \frac{1 - \nu_g^2}{E_g} \right)^2}{\frac{r_h r_g}{r_h + r_g} \nu} \right)^{\frac{1}{5}}$$
 (6)

By Substituting Eq. (3) into Eq. (1),  $E_d$  is written as follows:

$$E_d = \frac{Hr_c^2}{12\delta^2} \tag{7}$$

Thus, the *van der Waals* energy ( $E_{vdW}$ ) between two deformed particles is written as follow:

$$E_{vdW} = \frac{Hr_c^2}{12\delta^2} + \frac{H}{6\delta} \frac{r_h r_g}{r_h + r_g}$$
 (8)

# 2.2. Relative kinetic energy

Relative kinetic energy ( $E_{Kin}$ ) is given by:

$$E_{Kin} = \frac{1}{2}\,\hat{m}v^2\tag{9}$$

where  $\hat{m}$  stands for the relative mass, which is given by:

$$\hat{m} = \frac{m_h m_g}{m_h + m_g} \tag{10}$$

where  $m_h$  and  $m_g$  are the mass of host and guest particles respectively, and v is the relative velocity in Eq. (9). The Resonant Acoustic® Mixer (LabRAM) system utilizes a simple harmonic motion, and allows particles collide with each other when particles

are bounced from container walls. Thus, a very rudimentary estimate of the average relative velocity would be:

$$v = 2f \int_{0}^{\frac{1}{2f}} -\omega A \sin(\omega t) dt = -4Af$$
 (11)

where f is the frequency, which is 60 Hz in the LabRAM system and  $\omega$  is angular velocity. A is the amplitude of the vibration, which depends on load and intensity, and can be measured experimentally using a slow-motion camera. Alternately, the dry coating process can be computationally simulated using the discrete element method (DEM), which is highly suited for estimating such quantities, which may be considered in future investigations.

#### 2.3. Plastic deformation energy

Plastic deformation energy  $(E_p)$  is determined by [52]:

$$E_p = F\Delta s = F(s_g + s_h) \tag{12}$$

where  $s_g$  and  $s_h$  stand for the indentation depths of guest and host particles respectively (see Fig. 1), while F is the contact force computed according to Eq. (5). Also, Eq. (3) may be written as:

$$S = \pi \left[ r_g^2 - \left( r_g - s_g \right)^2 \right] = 2\pi r_g s_g - \pi s_g^2 = 2\pi r_h s_h - \pi s_h^2$$
 (13)

If the contact radii of host and guest particles were assumed much larger than their respective indentation depths  $(r_g \gg s_g \text{ and } r_h \gg s_h)$ , the contact area of two deformed particles can be calculated as:

$$S \approx 2\pi r_g s_g \approx 2\pi r_h s_h \tag{14}$$

Based on Eq. (14), the depth of coarse particle plastic deformation can be also calculated by:

$$s_h = \frac{r_g}{r_h} s_g \tag{15}$$

Based on Eqs. (3) and (14), the depth of fine particle plastic deformation can be calculated by:

$$s_g = \frac{r_c^2}{2r_\sigma} \tag{16}$$

Since  $r_h \gg r_g$ , from Eq. (15),  $s_g \gg s_h$ . Hence, Eq. (12) may also be written as:

$$E_p = F s_g = \frac{F r_c^2}{2 r_\sigma} \tag{17}$$

# 2.4. Deagglomeration energy

During the dry coating process, the large agglomerates of guest particles initially attach onto the surface of host particles to form a non-uniform coating. A uniform coating occurs after repeated collisions between particles as well as between particles and system components (vessel walls, etc.). Some guest particles escape from the agglomerates, leading to deagglomeration [14]. If the relative kinetic energy is larger than the deagglomeration energy, the guest agglomerates will be fragmented and individual guest particles will be well distributed on the surfaces of host particles. Otherwise, fine particles will remain as agglomerates. The energy needed for deagglomeration is the sum of *vdW* energy and plastic deformation. For the sake of simplicity, first order estimate can be made by considering interactions between a pair of guest particles. Consequently, Eq. (8) may be used after replacing the host

particle size with the guest particle size. The proposed equation for deagglomerate energy ( $E_{de}$ ) is:

$$E_{de} = \frac{Hr_c^2}{12\delta^2} + \frac{Hr_g}{12\delta} + \frac{Fr_c^2}{r_g}$$
 (18)

# 2.5. Estimation of guest attachment and deagglomeration energies

It is assumed that the total energy for detachment is the sum of vdW energy, plastic deformation energy and deagglomeration energy. If the total energy for detachment is larger than the relative kinetic energy, the guest and host particles will stick together. Otherwise, the guest particles will bounce off of the host particles [1]. Thus, the quality of dry powder coating can be assessed by using Eqs. 8, 9, 17 and 18. It is also useful to define the quality index of dry powder coating ( $K_c$ ), which is the ratio of total detachment energy to kinetic energy, given below:

$$K_c = \frac{E_{vdW} + E_p + E_{de}}{E_{kin}} \tag{19}$$

if  $K_c > 1$ , guest particles tend to stick on the host particles; if  $0 < K_c < 1$ , two particles tend to separate. Also, the quality index of deagglomeration  $(K_d)$  is defined as below:

$$K_d = \frac{E_{de}}{E_{bin}} \tag{20}$$

when  $K_d > 1$ , the agglomerates of guest particles tend to form more agglomerations, if  $0 < K_d < 1$ , guest particles tend be get better dispersed.

#### 3. Materials and methods

#### 3.1. Materials

Potassium Chloride (*KCl*), purchased from SIGMA-ALDRICH (St Louis, MO), was chosen to represent host particles and was pre-sieved into two size ranges (125–250 and 250–355  $\mu$ m). *KCl* is approximately spherical in shape, Fig. 2a. cornstarch (a micron-sized polymeric material), purchased from ACH Food Companies, Inc. (Memphis, TN), was

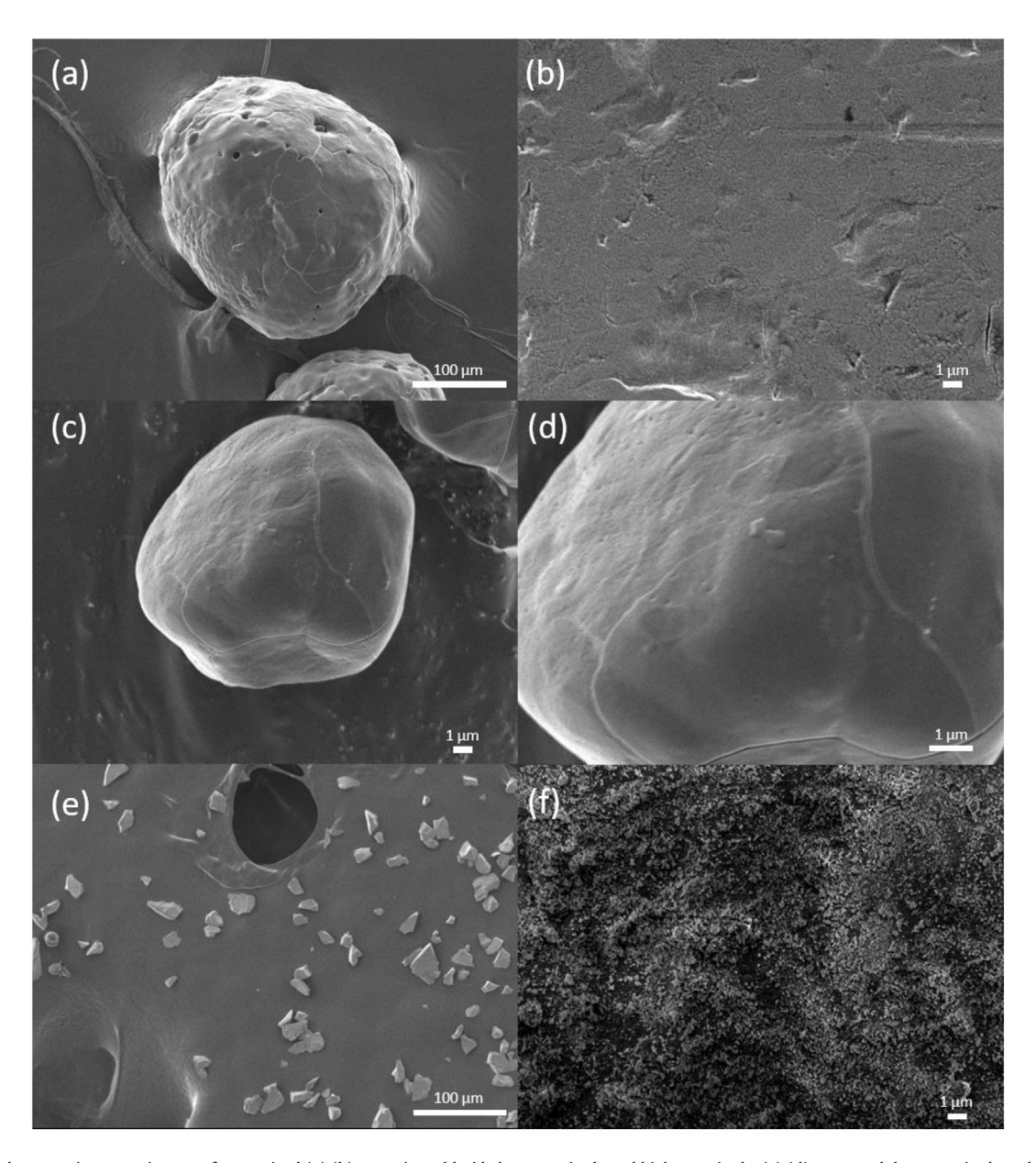


Fig. 2. Scanning electron microscopy images of as-received (a) (b) potassium chloride low magnitude and high magnitude, (c) (d) cornstarch low magnitude and high magnitude, (e) aluminum silicate and (f) Aerosil R972P.

**Table 1**Sieve cuts and corresponding size statistics for KCl, cornstarch, aluminum silicate and Aerosil R972P.

	Sieve Cut	$x_{10} (\mu \mathrm{m})$	x <sub>50</sub> (μm)	x <sub>90</sub> (μm)	$\rho  (\mathrm{kg}/\mathrm{m}^3)$	Poisson's ratio (-)	Young's modulus (GPa)	Hamaker constant $(10^{-20}\text{J})$
Host particle	Potassium chloride							
•	250-355 μm	234.73	329.52	458.94	1980	0.22	29.8	5.5
	125-250 μm	157.13	209.39	346.58	1980	0.22	29.8	5.5
Host and Guest particle	Cornstarch							
	As received	6.85	14.91	23.66	1550	0.30	0.04	6.3
Guest particle	Aluminum silicate							
	<25 μm	8.87	18.20	32.17	2350	0.26	112.3	15
	Aerosil R972P							
	As received		0.02		2650	0.17	73.1	6.5

**Table 2**Formulations for host and guest particles for the investigation of the effect of material hardness.

Host particle	Guest particle	Mass of host particle (g)	Mass of guest particle (g)	Theoretical surface coverage (%)
Potassium chloride 125–250 μm	Cornstarch	12.265	2.735	100
Potassium chloride 125–250 μm	Aluminum silicate	10.618	4.382	100

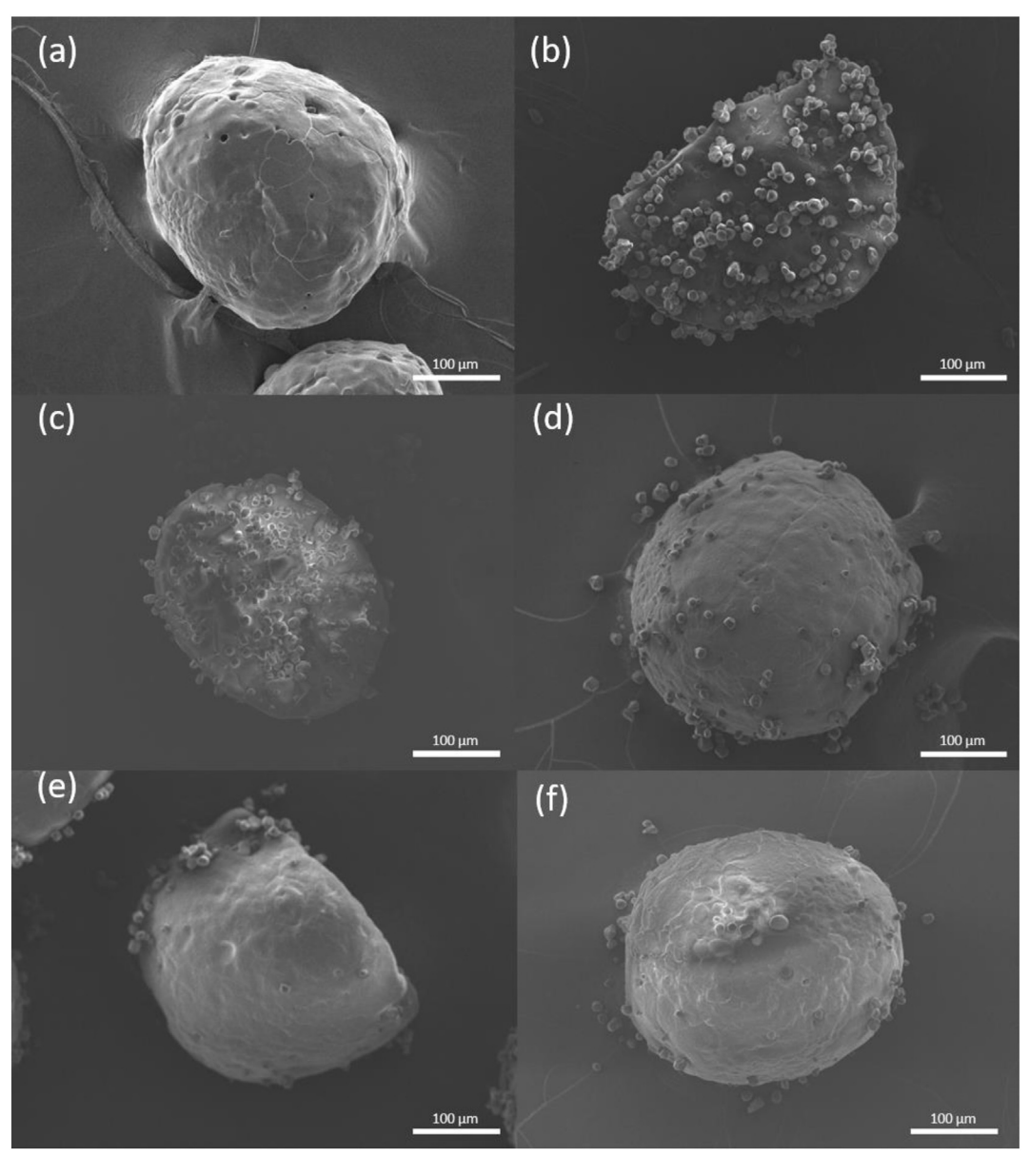


Fig. 3. SEM images of (a) 125–250  $\mu$ m KCl coated with cornstarch processed at: (b) 10 Gs (c) 30 Gs, (d) 50 Gs, (e) 70 Gs, (f) 90 Gs.

used to represent either guest (coarse) or host (fine) particles. Aerosil R972P is a nano-sized pharma-grade hydrophobic silica from Evonik (Parsippany, NJ), and was chosen to represent fine (guest) particles. Aluminum silicate powder with an irregular particle shape, purchased from SIGMA-ALDRICH (St Louis, MO), was chosen to represent a third guest particle, which was also pre-sieved to narrow the particle size distribution and reduced  $D_{50}$  of 18  $\mu$ m. The particle sizes and properties of materials are provided in Table 1.

#### 3.2. Methods

# 3.2.1. Dry coating process

In these experiments, the amount of guest materials to be used for dry coating is selected based on a 100% theoretical surface area coverage. *Yang* et al, [53] suggested the following equation as a theoretical weight percentage of guest particles for 100% surface area coverage of host particles:

$$G_{wt}\% = \frac{4r_g\rho_g}{4r_g\rho_g + r_h\rho_h} \times 100\% \tag{21} \label{eq:21}$$

where  $r_h$ ,  $r_g$ ,  $\rho_h$  and  $\rho_g$  are the particle radii and densities of host and guest particles respectively. In total, 15 g mixture of host particles (KCl or cornstarch) and guest particles (cornstarch, aluminum silicate or Aerosil R972P) were blended in a cylindrical polycarbonate jar with height of 5.33 cm, inner diameter of 5.72 cm, and total volume of 135 cm<sup>3</sup>. The dry coating results may be impacted by the tribocharging properties of the jar material since some of the guest particles may get attached. However, since the total surface areas of the vessel is much smaller than that of the host particles, the results are expected to be not that significantly impacted. Besides, in practical applications, additional care may be taken to utilize the jar/vessel materials that promote lesser charging and sticking. The Laboratory Resonant Acoustic Mixer (LabRAM) (Resodyn Acoustic Mixers, Inc. MT), a high-intensity vertical vibrational mixer, was used for mixing and coating. The LabRAM has been proven to be capable of breaking up particulate agglomerates, and distributing the guest particles on to the surface of host particles via high shear forces [26]. The vibration intensities were varied from 30 to 90 times the acceleration of gravity (Gs). The vibration frequency was fixed at 60 Hz, and the processing time was fixed at 5 min, which are the same as previous literature [26,34]. After coating process, all

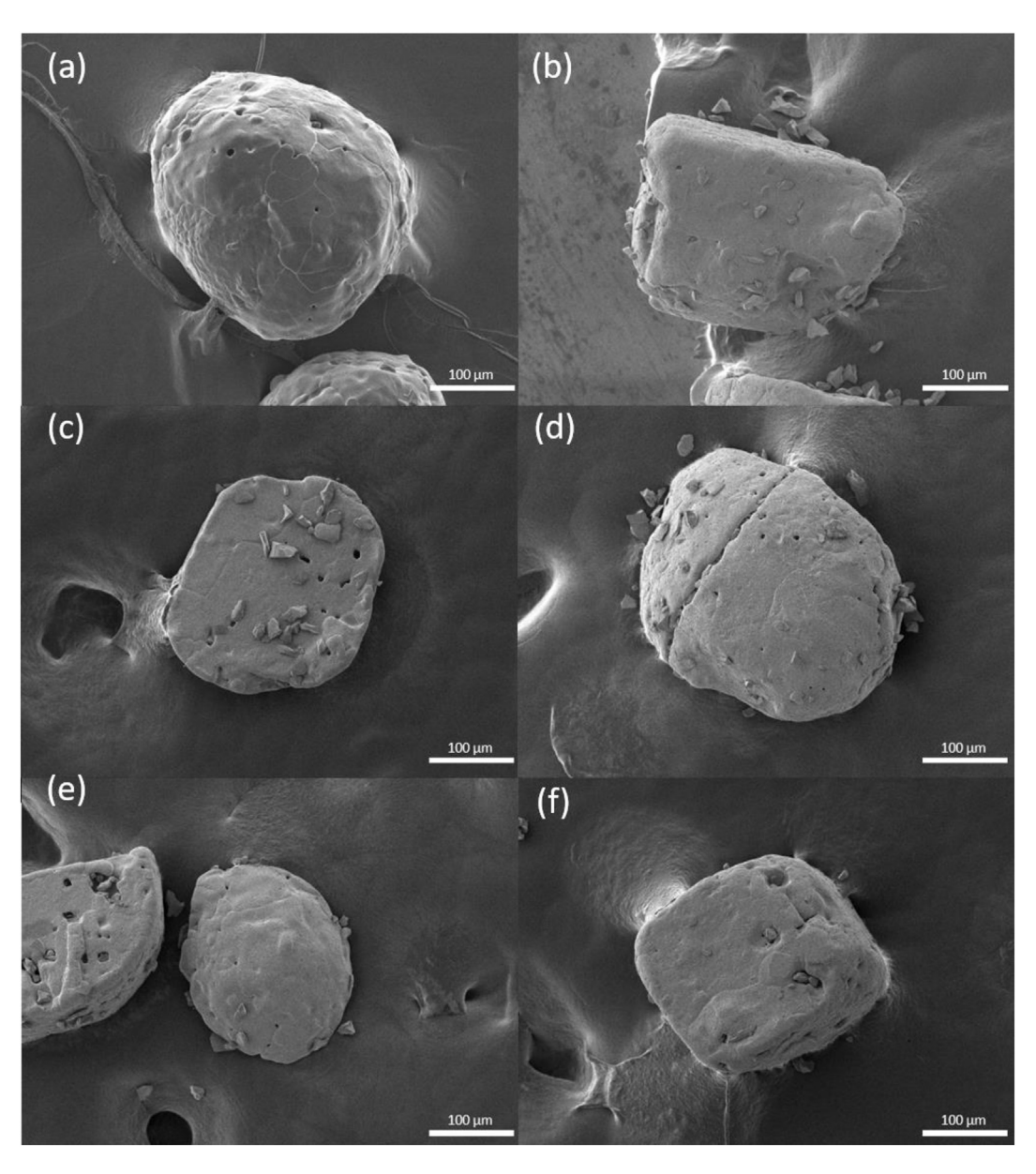
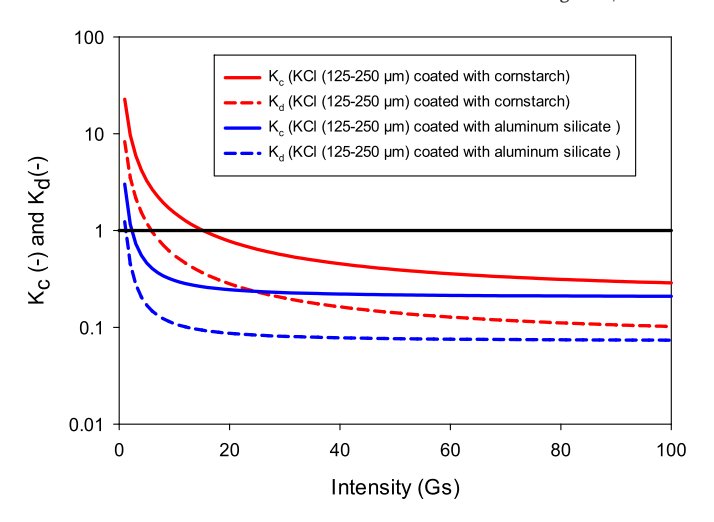


Fig. 4. SEM images of (a) 125–250 µm KCl coated with aluminum silicate at: (b) 10 Gs (c) 30 Gs, (d) 50 Gs, (e) 70 Gs, (f) 90 Gs.



**Fig. 5.** Performance indices for dry coating  $(K_c)$  and de-agglomeration  $(K_d)$  for the coating quality assessment of 125–250  $\mu$ m KCl coated with cornstarch or aluminum silicate.

samples were stored at room temperature of  $25\,\mathrm{C}$  along with the relative humidity between 25 and 35%.

#### 3.2.2. Helos/Rodos particle sizer

The particle size distributions of materials were evaluated via Sympatec RODOS/HELOS laser diffraction particle size analyzer (Sympatec Inc. NJ). 1–2 g of powder samples were fed into dry dispersion feeder system, and 0.5 bar dispersion pressure was used to ensure adequate particle dispersion without chance of particle breakage. The cumulative particle size distributions were calculated using the Sympatec Windox 5.0 software. Particle size measurements for each sample were repeated 3 times and average results are used. Further details can be found in the previous literature [22].

#### 3.2.3. True density

The true (particle) density of the materials was measured with the Multipycnometer true density analyzer (P/N 02029–1, Quantachrome Instruments, FL). Measurements were taken using Helium gas for each sample and the average of 5 density measurements are reported.

# 3.2.4. Scanning Electron Microscopy

The coating quality of guest particles onto the surface of host particles was qualitatively examined using JSM-7900F Field Emission Scanning Electron Microscopes (SEM) (JEOL USA, Inc. MA). The beam energy was varied (1–3 kV) for different samples. Powder samples were pre-coated with Carbon via a sputter coater (Q150T 16,017, Quorum Technologies Ltd., Laughton, East Sussex, England) to prevent the

**Table 3** Material properties used in the model.

Parameter	Value	Unit
Hamaker constant (H)	$1 \times 10^{-19}$	J
Atomic scale separation $(\delta)$	0.165	nm
Frequency of vibration (f)	60	Hz
Poisson's ratio of guest particle $(\nu_g)$	0.25	-
Poisson's ratio of host particle $(\nu_h)$	0.25	_
Young's modulus of host particle $(E_h)$	50	Gpa
Young's modulus of guest particle $(E_g)$ (section 4.2 and 4.3)	50	Gpa
Density of guest particle $(\rho_g)$	2000	Kg/m <sup>3</sup>
Density of host particle $(\rho_h)$	2000	Kg/m <sup>3</sup>
Amplitude (1 to 100 Gs) (A)	$6.9 \times 10^{-3}$ to $6.9 \times 10^{-1}$	cm

accumulation of static electric fields, to improve image contrast and to enhance conductivity under SEM [25].

#### 4. Results and discussion

In this section, the influence of guest particle stiffness (section 4.1), guest particle size (section 4.2), and host particle size (section 4.3) are investigated and the corresponding results are discussed. In each case, the effect of the processing intensity being a major factor is also examined.

# 4.1. Effect of guest particle stiffness

Material properties of particles may have a significant effect on the coating quality [12,48,53]. Stiffness, represented by *Young*'s modulus (Elastic modulus), of guest particles can affect coating performances, even if the materials are processed under the same conditions. Cornstarch and aluminum silicate were selected as guest parties to investigate the stiffness effect on the dry coating process. Formulations of the guest and host particles are listed in Table 2. The corresponding estimated theoretical surface area coverages of host particles are kept at 100%, although the guest particles weight percentages are not the same, which is due to the differences of guest particle sizes.

As shown in Table 1, cornstarch and aluminum silicate have the similar particle size distributions, yet have large differences in Young's modulus. Compared to aluminum silicate, cornstarch is a powder that could be more easily deformed during collision. Fig. 3 depicts KCl (125–250 μm) coated with cornstarch via LabRAM under the processing conditions of 10 Gs to 90 Gs. Guest particle numbers and surface area coverage could be an effective way to evaluate dry coating performance. For comparison, SEM images of as-received KCl are shown in Fig. 2a and b at low and high magnifications respectively. In Fig. 3, it is clear to see that the number of cornstarch particles attached to the surface of KCl decreased with increasing mixing intensity. When mixing intensity was set at 10 and 30 Gs (Fig. 3b and c), the cornstarch particles are well dispersed onto the surface of KCl. On the contrary, only a few cornstarch particles were observed on the surface of KCl when the mixing intensity was set to 70 Gs (Fig. 3e) or 90 Gs (Fig. 3f). In addition, although most of cornstarch particles were distributed on the surface of KCl particle, some cornstarch agglomerates still could be seen in all cases of the mixing intensity from 10 to 70 Gs (Fig. 3b, c, d and e). However, the number of cornstarch agglomerates reduced with increasing intensity, especially in 90 Gs case (Fig. 3f). Additional SEM and optical microscopy images and results of quantitative analysis of the surface area coverage for this case are included in the supplementary materials.

Next, KCl was dry coated with aluminum silicate, a guest particle which has similar particle size as cornstarch, but much higher Young's Modulus. As shown in Fig. 4, after mixing KCl (125–250  $\mu$ m) and aluminum silicate at the mixing intensities of 10 to 90 Gs for 5 min, only small amounts of aluminum silicate particles were observed on the surface of KCl at 10 and 30 Gs (Fig. 4b and c), but as the intensity increases, there hardly any particles; i.e., just a few at 50 Gs (Fig. 4e). These results show that aluminum silicate is not a good guest particle to use for dry coating process as compared to cornstarch, and indicates higher guest material stiffness results in poor coating quality in this situation. Additionally, coating performance worsens with increasing mixing intensity, which was also the case for cornstarch. Interestingly, aluminum silicate agglomerates were not observed in any of the SEM images in Fig. 4. With regards to the effect of process intensity, in both cases, the coating performance deteriorated with increasing mixing intensity. This means that higher intensity does not always provide better coating quality, especially for larger guest particle sizes. In contrast, agglomeration tendency reduced with the increasing intensity and stiffness. Additional SEM and optical microscopy images and results of quantitatively analysis of the surface area coverage for this case are included in the supplementary materials.

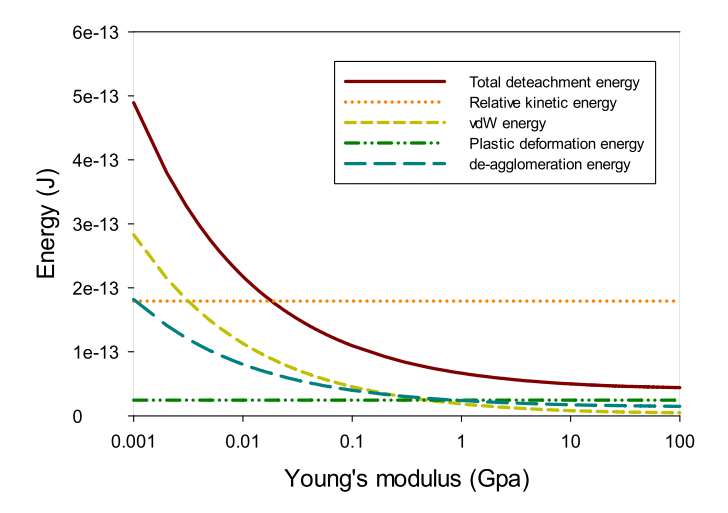


Fig. 6. Material stiffness effect on interparticle energies when processed at 50 Gs.

The above experimental results may be explained using the stick/bounce model. First, quality indices for dry coating ( $K_c$ ) and deagglomeration ( $K_d$ ) were calculated as a function of vibration intensity for KCl (125–250  $\mu$ m) coated with either cornstarch or aluminum silicate, shown in Fig. 5. All the parameters in the model, which are listed in Tables 1 and 3, were either obtained from the material manufacturer or the previous studies [5,28,43,46]. It is noted that one could obtain more accurate estimates for some of these but for the purpose of illustrating the major trends, the values used are adequate. Using these characteristic parameters and the energy-based stick/bounce model, the dry powder coating index  $K_c$  as calculated using vdW, plastic deformation, deagglomeration and relative kinetic energies according to Eq. (19). The deagglomeration index  $K_d$  was calculated using deagglomeration

**Table 4**Formulations of host and guest particles for the investigation of the effect of guest particle size

Host particle	Guest particle	Mass of host particle (g)	Mass of guest particle (g)	Theoretical surface coverage (%)
Potassiumchloride 125–250 µm	Aluminum silicate	10.618	4.382	100
Potassium chloride 125–250 µm	Aerosil R972P	14.992	0.008	100

and relative kinetic energies according to Eq. (20). K<sub>c</sub> decreased with increasing intensity using either guest material, indicating that guest particles tend to bounce off of the host particles at high processing intensity. In addition,  $K_c \ge 1$  occurs for the intensities below 16 Gs and 3 Gs for cornstarch and aluminum silicate respectively. This indicates good coating performances would be reached when using processing intensities below these values, for the respective guest materials, although it is possible that such low intensities may not provide adequate mixing action between the host and guest materials. Lower  $K_c$  values indicate poorer coating performances. The coating performances observed in Figs. 3 and 4 are in line with model estimations in Fig. 5. When KCl was coated with cornstarch particles, the best coating performance was attained when processed at 10 Gs. However, KCl particles were not well coated at 70 Gs and 90 Gs, since these intensities are much higher than the 16 Gs threshold. Although aluminum silicate was not well coated on KCl particles, even at the lowest processing condition, such a result should be expected since the maximum intensity to attain  $K_c \ge 1$  is 3 Gs. To assess guest particle agglomeration tendency,  $K_d$ values were computed and found to be less than 1 (indicating adequate deagglomeration of guest particles) above 6 Gs and 1 Gs for cornstarch and aluminum silicate respectively, shown in Fig. 5. The lower  $K_d$  value

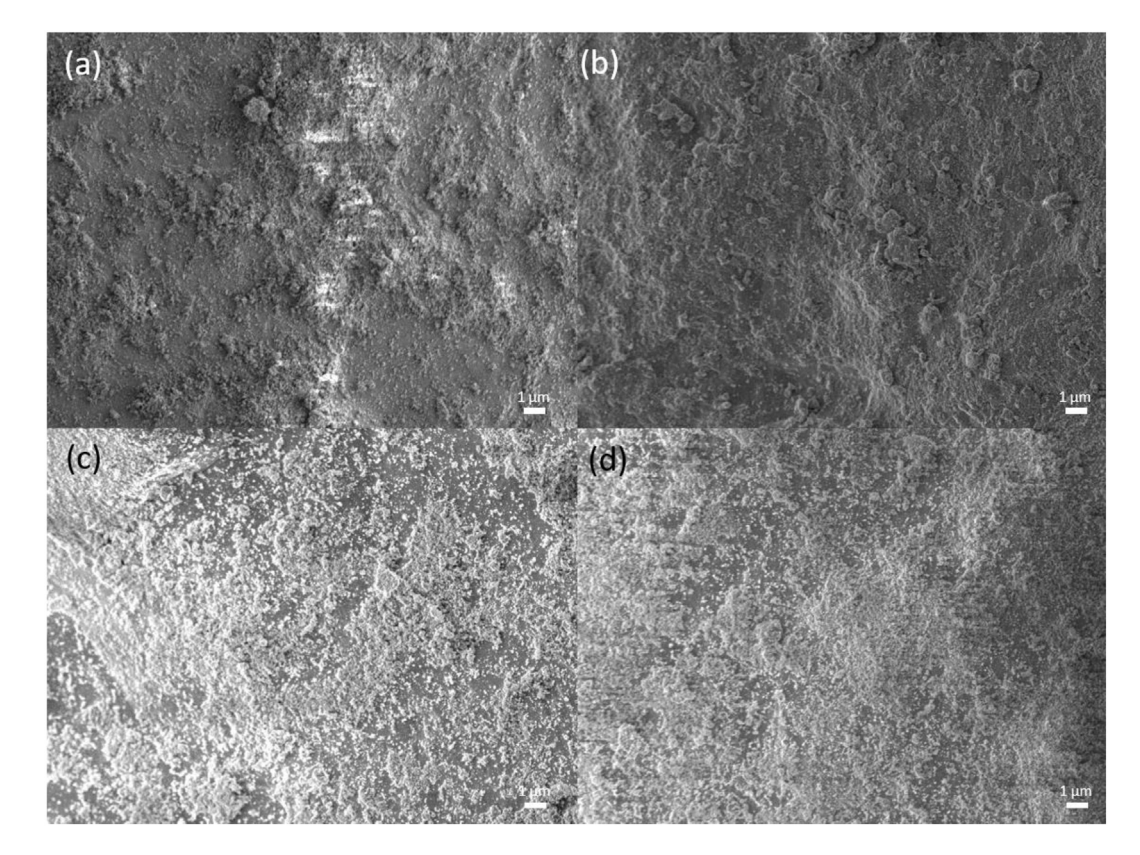
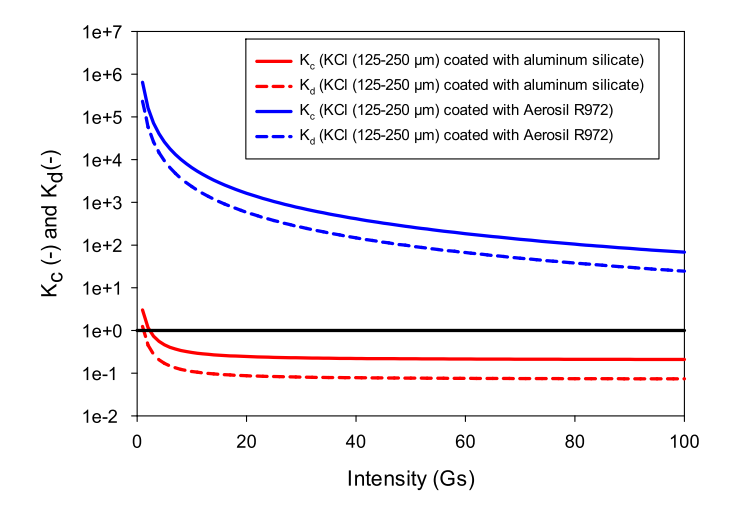


Fig. 7. SEM images of 125-250 µm KCl coated with Aerosil R972 processed at: (a) 30 Gs, (b) 50 Gs, (c) 70 Gs, (d) 90 Gs.

means the better deagglomeration performance. From the experimental observations, only small amounts of guest agglomerations were observed especially for high intensities cases. These simulated results using the proposed model corroborate the experimental observations, validating the use of stick/bounce model for estimating the coating performance.

Next, the stick/bounce model was used to evaluate the effect of guest particle stiffness (Young's modulus) on dry coating performance. The simulated results are plotted in Fig. 6 for the Young's modulus of guest particles ranging from 0.001 to 100 GPa. In this figure, the radius of guest and host particles was fixed at 5 µm and 100 um respectively, which generally mimic the particle sizes of cornstarch, aluminum silicate and KCl. The mixing intensity was fixed at 50 Gs, and the other parameters used in the model (Hamaker constant, atomic scale separation, etc.) are listed in Table 3. Fig. 6 shows that the total detachment energy decreased with increasing Young's modulus, indicating that the guest particles have an increasing tendency to bounce off the host particles as they become harder. It is noted that the relative kinetic energy stayed constant as expected because as per Eq. (9) kinetic energy is independent of Young's modulus. When the Young's modulus value is 0.02 Gpa, the total detachment energy equals to relative kinetic energy. This indicates that it is recommended to use guest particles with Young's Modulus below 0.02 GPa in order to attain adequate coating quality when processed at 50 Gs. That is corroborated by the experimental results where the coating quality of cornstarch was better than that of aluminum silicate when processed under 50 Gs, since the Young's Modulus of cornstarch is much closer to 0.02 GPa. As shown, the vdW energy and the deagglomeration energy both decrease with increasing stiffness. This is due to the fact that higher Young's modulus leads to smaller indentation depths, as well as contact areas. In other words, more ductile guest particles will have larger indentation depths, and more energy is needed to separate particles. In general, harder guest particles require less energy to bounce off from each other, indicating a lower Young's modulus is favorable for the coating and providing better coating performances, unless the host particle has a very low stiffness. On the contrary, a higher Young's modulus of the guest particles is favorable for deagglomeration, which is observed in the experimental results. The interesting finding is that the plastic deformation energy remained relatively constant. This can be attributed to the fact that increased Young's modulus, based on Eqs. 5 and 6, increases the collision force, decreases the collision time, and also decreases the indentation depth at the same time. These changes cancel out, resulting in relatively net zero change in plastic deformation energy.



**Fig. 8.** Performance indices for dry coating  $(K_c)$  and de-agglomeration  $(K_d)$  for the coating quality assessment of 125–250  $\mu$ m KCl coated with aluminum silicate or Aerosil R972.

# 4.2. Effect of guest particle size

The dry powder coating experiments were carried out with KCl  $(125-250\,\mu\text{m})$  as host particles and either aluminum silicate or Aerosil R972P as guest particles, at 30 to 90 Gs mixing intensity. The material properties of host and guest particles are listed in Table 1. Both aluminum silicate and Aerosil R972P have high stiffness, but two orders of magnitude difference in their particle size, making it possible to investigate the effect of guest particle size on dry particle coating. Theoretical weight percentage of guest particles to attain 100% surface area coverage of host particles (KCl) was used and these values are displayed in Table 3.

The SEM images of KCl ( $125-250~\mu m$ ) coated with either aluminum silicate or Aerosil R972P are shown in Figs. 4 and 7 respectively. Formulations of the guest and host particles are listed in Table 4. In Fig. 4, as discussed in the previous section, SEM images display general poor coating quality with aluminum silicate, which gets worse with increasing processing intensity. On the other hand, Aerosil R972P nano-silica particles easily attach to KCl particles as seen in Fig. 7, at processing conditions from 30 Gs to 90 Gs. However, the SEM images in Fig. 7 also show that KCl surfaces are not fully covered and Aerosil R972P agglomerates can be observed. Results of optical microscopy images and quantitative analysis of the surface area coverage for this case are included in the supplementary materials. Also, increasing processing intensity appears to have no detrimental effect on coating quality in the Aerosil R972P cases.

These results may be explained using the model. First, the dry coating  $(K_c)$  and deagglomeration  $(K_d)$  quality estimations are plotted in Fig. 8 as a function of vibration intensity for KCl (125–250  $\mu$ m) coated with either aluminum silicate or Aerosil R972P.  $K_c \ge 1$  indicates guest particles tend to stick to host particle surfaces, while  $K_c < 1$  indicates that guest particles will tend to bounce off the surface of host particles upon a collision event. For KCl coated with Aerosil R972P, it can be observed that  $K_c \ge 1$  for all mixing intensities, indicating that Aerosil R972P nano-silica would stick onto the surface of KCl host particles at these intensities. On the other hand, as mentioned in the previous section, the coating performance of aluminum silicate was not good when processed using 30 Gs to 90 Gs. In terms of guest agglomeration,  $K_d$  decreased with increasing mixing intensity in both cases, indicating improved deagglomeration with increasing mixing intensity. However, even at 90 Gs,  $K_d$  is still much larger than 1 for Aerosil R972P, implying that guest particle agglomeration is expected even at high vibration intensities. In summary, the stick/bounce model predicts that guest Aerosil R972P particles would stick on the host KCl particles, and that some agglomeration of guest particles would be expected, regardless of which vibration intensity is used. These model-based predictions corroborate and explain the experimental results shown in Fig. 7.

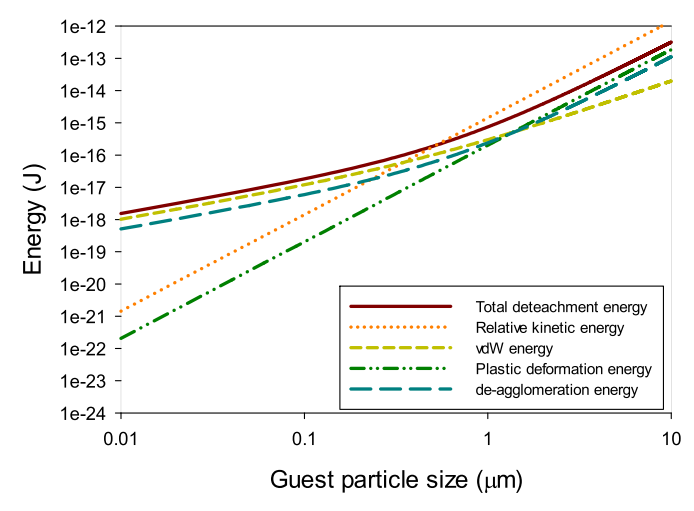


Fig. 9. Guest particle size effect on interparticle energies when processed at 50 Gs.

**Table 5**Formulations of host and guest particles for the investigation of the effect of host particle size

Host particle	Guest Particle	Mass of host particle (g)	Mass of guest particle (g)	Theoretical surface coverage (%)
Potassium chloride 250–355 µm	Cornstarch	13.139	1.861	100
Potassium chloride 125–250 µm	Cornstarch	12.265	2.735	100
Potassium chloride 125–250 µm	Aerosil R972P	14.992	0.008	100
Cornstarch	Aerosil R972P	14.864	0.136	100

Next, simulated results using the model for the fixed radius of host particles (100 µm) and mixing intensity of 50 Gs are shown in Fig. 9, where the guest particles size ranged from 0.01 µm to 20 µm, which covers the size of KCl, Aerosil R972P and aluminum silicate. The characteristic parameters used are summarized in Table 3. The results shows that as the guest particle size increases, the total detachment energy  $(E_{tot})$  is higher than the relative kinetic energy  $(E_{kin})$ when the guest particle size is less than 0.5 µm, indicating that guest particles below 0.5 µm would stick onto the surface of host particles. On the other hand, guest particles larger than 0.5 µm would tend to bounce off of the host particles. As the guest particle size increases, the relative kinetic energy  $(E_{kin})$  increases much faster than the other energies, which indicates  $E_{kin}$  is more sensitive to guest particle size. Further,  $E_{kin}$  is lower than the deagglomeration energy ( $E_{de}$ ) for guest particles below 0.25 µm, implying those guest particles tend to form agglomerates. In addition,  $E_{tot}$ , as well as all other energies increase with increasing guest particle size. Larger sized guest particles lead to higher collision forces, resulting in larger deformation/contact area of particles. Eqs. 7 and 17 indicates that larger deformation means higher vdW energy  $(E_{vdW})$  as well as plastic deformation energy  $(E_p)$ . An interesting

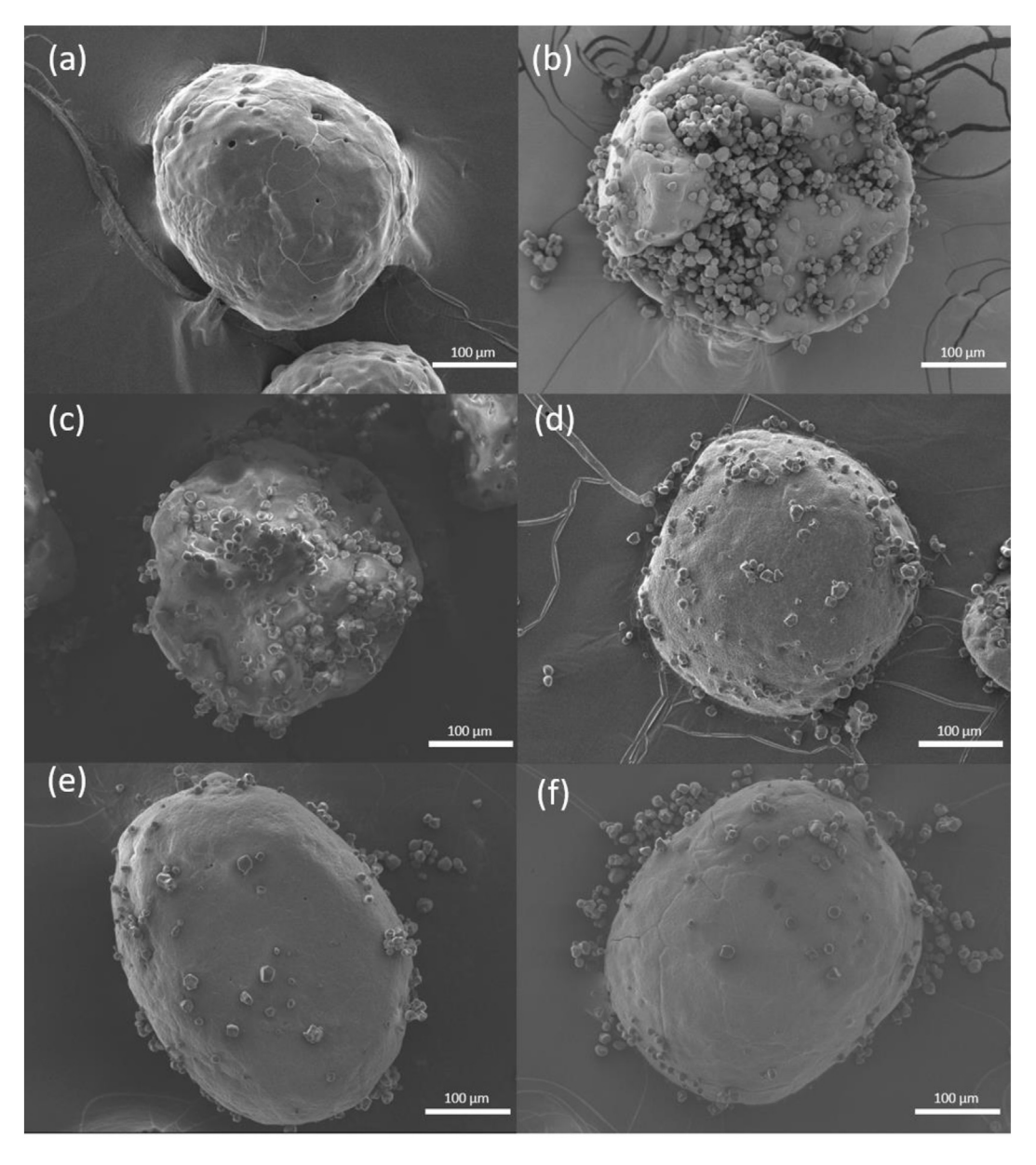
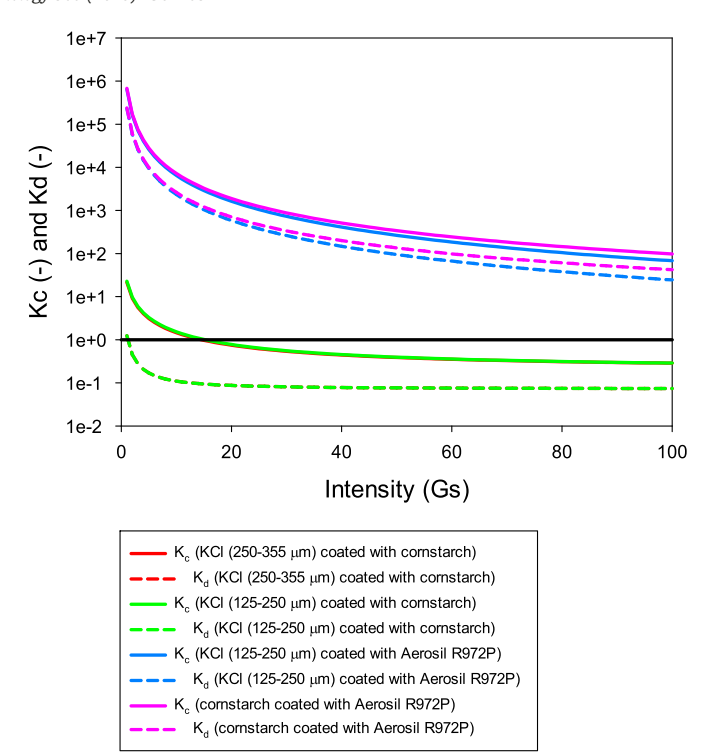


Fig. 10. SEM images of (a) 250-355 µm KCl coated with cornstarch at: (b) 10 Gs (c) 30 Gs, (d) 50 Gs, (e) 70 Gs, (f) 90 Gs.

phenomenon is that the total detachment energy ( $E_{tot}$ ) is dominated by vdW energy for smaller guest particle sizes (less than ~1.4 µm), while it is dominated by the deagglomeration energy for larger guest particle sizes (larger than 1.4 µm). This indicates that the deagglomeration step consumes the most energy when the guest particles are in the micron size range (1 µm or larger). This phenomenon was also observed by others [16,41]. In summary, the nano and sub-micron sized guest particles (less than 1 µm) would lead to higher tendency for guest particle agglomeration, while larger micro-sized guest particle size would lead to the separation of host and guest particles during the dry powder coating process. In other words, using relatively higher processing intensities and/or larger guest particle sizes may lead to poor dry powder coating when using micro-sized guest particles.

# 4.3. Effect of host particle size

Here, two sizes of KCl (125–250  $\mu$ m and 250–355  $\mu$ m) and cornstarch were used to investigate the host particle size effect on dry coating performance. Both micro-sized (cornstarch) and nano-sized (Aerosil R972P) guest particles were considered. KCl (125–250 µm) and KCl (250–355  $\mu$ m) were coated with micro-sized cornstarch at mixing intensities from 10 Gs to 90 Gs. In addition, KCl (125–250  $\mu$ m) and cornstarch were coated with nano-sized Aerosil R972P processed from 30 Gs to 90 Gs. The properties and conditions are shown in Table 5. Coating performances of KCl (250–355 μm) coated with cornstarch are shown in Fig. 10. Compared with Fig. 3, the surface area coverages of KCl coated with cornstarch deteriorated with increasing mixing intensity in both cases, demonstrating a similar trend of coating quality. In addition, most cornstarch particles were well distributed on the surface of KCl particles, only small agglomerates were observed from SEM images in both cases. For the cases where KCl (125-250 μm) or cornstarch were coated with Aerosil R972P, the coating qualities are shown in Figs. 7 and 11 respectively. Similar observations were found as well in both cases. Aerosil R972P attaches to the host particles



**Fig. 12.** Performance indices for dry coating  $(K_c)$  and de-agglomeration  $(K_d)$  for the coating quality assessment.

of KCl at all processing conditions, although the guest particles did also form agglomerates. The comparisons between all cases demonstrate that the host particle size ranges considered here had a minor effect on the coating quality.

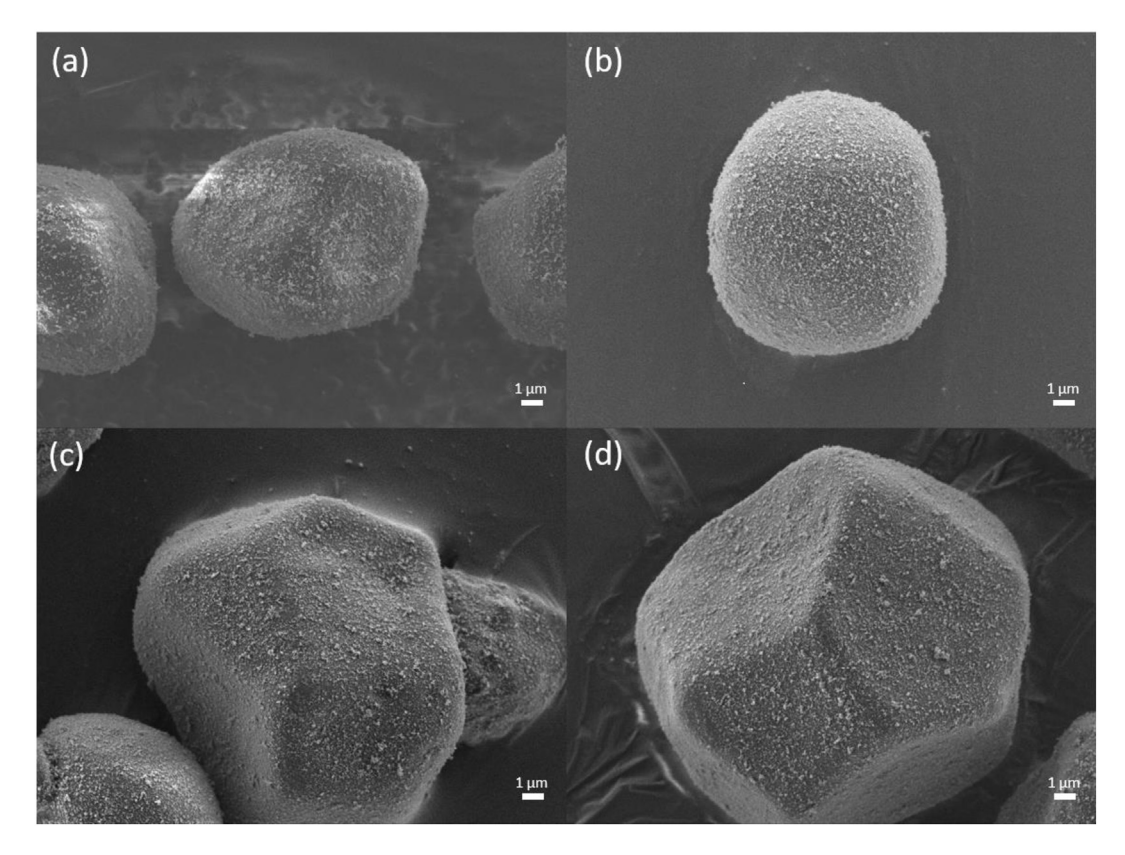


Fig. 11. SEM images of cornstarch coated with Aerosil R972 processed at: (a) 30 Gs, (b) 50 Gs, (c) 70 Gs, (d) 90 Gs.

These results may be explained using the model to estimate the dry coating  $(K_c)$  and deagglomeration  $(K_d)$  quality indices and shown in Fig. 12.  $K_c$  and  $K_d$  decreased with the increasing intensity in all four cases. The values of  $K_c$  and  $K_d$ , in cases of KCl (125–250  $\mu$ m) and KCl  $(250-355 \mu m)$  coated with micro-sized cornstarch, nearly overlapped with each other and only minor differences could be seen. In both cases,  $K_c \ge 1$  when mixing intensity is 16 Gs or lower, indicating cornstarch particles tend to stick on the surface of KCl when processed below 16 Gs. It is also observed that guest agglomerates tend to be broken up if 6 Gs or larger intensity is used, since  $K_d \ge 1$  in these cases, as validated from SEM images of Figs. 3 and 10. However, lesser agglomeration by itself is not useful if the guest particles tend to bounce off. Therefore, the best coating occurs at intensities under 10 Gs. In addition,  $K_c$  and  $K_d$  values overlapped when KCl (125–250  $\mu$ m) and cornstarch were coated with Aerosil R972P, due to the high  $K_c$  and  $K_d$  values (much higher than 1) in both cases, the particles of nano-sized silica agglomerates were well dispersed onto the different sized host particles as seen in Figs. 7 and 11. Such trends were also observed in previous studies [12,25]. Overall, the model-based results agree with the experimental data, validating the stick/bounce model.

The stick/bounce model was also used to evaluate the effect of host particle sizes, ranging from 10  $\mu$ m to 1000  $\mu$ m on dry coating performance. Two guest particle sizes, 0.02  $\mu$ m and 10  $\mu$ m, are considered to mimic the size of KCl, Aerosil R972P and aluminum silicate, while mixing intensity is fixed at 50 Gs and Table 3 shows other properties and conditions. The model-based results are plotted in Fig. 13, which shows that when using 0.02  $\mu$ m guest particle size, only very minimal

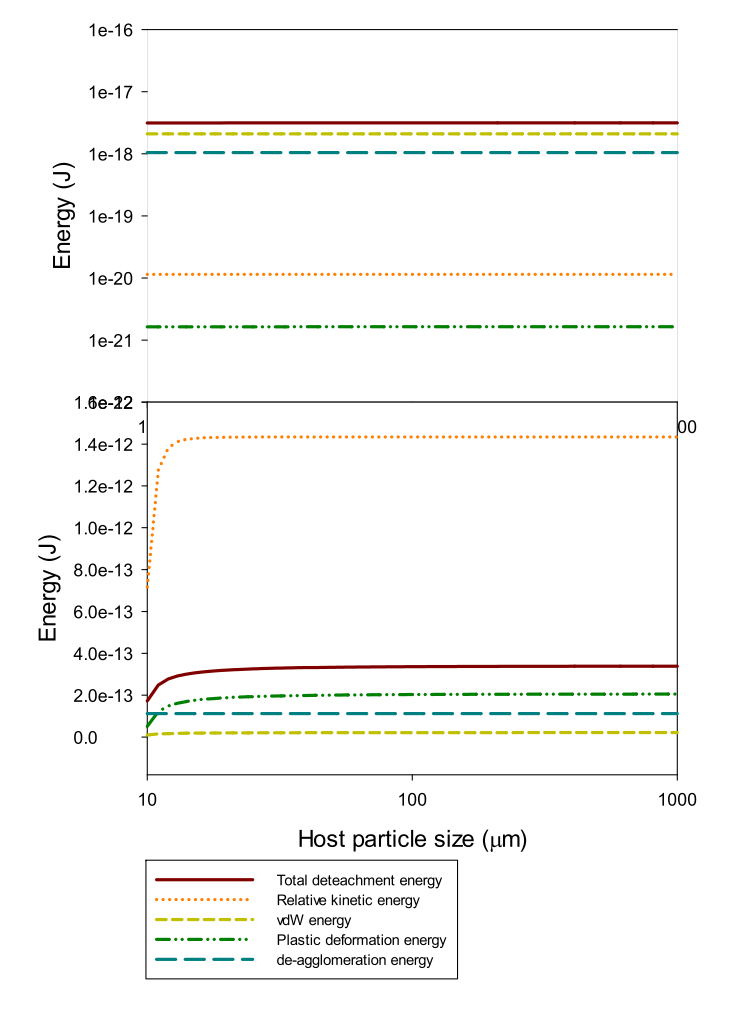


Fig. 13. Host particle size effect on interparticle energies when processed at 50 Gs with guest particle size of 0.02  $\mu m$  (top) and 10  $\mu m$  (bottom).

change in all types of energies could be observed. Thus, the host particle size has minor effect on the performance of dry coating, particularly when the host particle size is orders of magnitude larger than the guest particle size. This is evident from Eq. (10) for the effective mass of a pair of host-guest particles, which becomes mainly a function of the guest particle mass. That could explain why nano-sized silica has been successfully used in diverse examples of dry coating [10,12,20,25,31,34,53]. On the other hand, if the guest particle size and host particle size are in the similar range, i.e., guest particle size is less than or about one order of magnitude of host particle size, total detachment energy, relative kinetic energy, vdW energy as well as plastic deformation energy all increase with increasing host particle size, especially relative kinetic energy. In summary, for particles coated with micro-sized guest particles, the success of dry coating is not guaranteed, and the proposed stick/bounce model could be utilized to select proper coating materials as well as processing conditions.

#### 5. Conclusion

The effect of material stiffness and guest/host particle sizes along with mixing intensity on dry powder coating effectiveness was investigated. In terms of the stiffness, cornstarch as soft guest particles were well distributed and coated on the host particles of KCl (125-250 µm) at 30 Gs, with only few guest cornstarch agglomerates observed when the processing intensity varied from 30 Gs to 90 Gs. On the other hand, micro-sized aluminum silicate as harder guest particles tended to bounce off of host KCl particles, even at low processing intensity. In terms of the effect of guest particle size, nanosilica tended to attach onto the surface of host particles in all cases, achieving good dry coating quality, although the guest particles formed some agglomerates. The host particle size was found to have no significant effect on the coating quality when it is orders of magnitude larger than that of guest particles. For both types of micro-sized guest particles, increasing processing intensity led to guest particles bouncing off of host particles, indicating poor coating performance. On the contrary, higher mixing intensity may help decrease the agglomeration of micro-sized guest particles and could result in better coating quality. Such contradictory trends suggest that the best processing intensity would have an optimum range, and for example, in case of cornstarch coated with KCl (125-250 μm) it would be in the range 6 Gs to 15 Gs. When the guest particles are nano-sized, the impact of mixing intensity is lesser in terms of their attachment to host particles, which is in line with numerous previous experimental investigations involving nano-sized guest particles. The energy-based stick/bounce model was proposed to explain such experimental behavior and provides predictive ability for the design of coating system and processes. The model results corroborated the experimental results for dry coating of KCl with cornstarch, aluminum silicate and Aerosil R972 particles, which also validate the model. The coating index  $K_c$  was found to be a key model parameter which could be used to identify the dominant interaction energy between particles. When  $K_c > 1$ , good adhesive mixing is likely, while  $K_c$ <1 indicated poor adhesive mixing. The larger the  $K_c$  value, the better the coating performances, assuming that the processing time is long enough. In addition, the deagglomeration index  $K_d$  was another key model parameter which could be used to judge the deagglomeration tendency of guest particles, where  $0 < K_d < 1$  indicated good deagglomeration. Overall, it was found that the coating effectiveness is strongly correlated to the mixing intensity in conjunction with the material stiffness and guest particle size. The proposed energy-based stick/bounce model matched these trends well and could be used in the predication of dry coating performance, which could help better design the dry coating process and determining when not to use high mixing intensities.

#### **Notation**

Young's modulus of guest particle  $E_g$ Young's modulus of host particle  $E_h$ 

F contact force

Н Hamaker constant

relative mass m

mass of host particle  $m_h$ 

mass of guest particles  $m_g$ 

 $r_c$ contact radius

radius of guest particle rg

radius of host particle  $r_h$ 

S contact area

collision time 1/ is the relative velocity

#### Greek letters

t

atomic scale separation

Poisson's ratio of guest particle  $\nu_{\rm g}$ 

 $\nu_h$ Poisson's ratio of host particle

#### **Declaration of Competing Interest**

The authors declare that they have no known competing financial interests or personal relationships that could have appeared to influence the work reported in this paper.

### Acknowledgements

The authors gratefully acknowledge financial support from the National Science Foundation through grants EEC-0540855 and IIP-1919037.

# Appendix A. Supplementary data

Supplementary data to this article can be found online at https://doi. org/10.1016/j.powtec.2020.02.059.

# References

- [1] N. Almohammed, M. Breuer, Modeling and simulation of agglomeration in turbulent particle-laden flows: a comparison between energy-based and momentum-based agglomeration models, Powder Technol. 294 (2016) 373–402.
- M. Alonso, F. Alguacil, Dry mixing and coating of powders, Rev. Metal. 35 (1999).
- [3] M. Alonso, M. Satoh, K. Miyanami, Mechanism of the combined coatingmechanofusion processing of powders, Powder Technol. 59 (1989) 45-52.
- [4] L.E. Beach, Effect of dry particle coating on the properties of cohesive pharmaceutical powders, PhD thesis, 2011.
- [5] L. Bergström, Hamaker constants of inorganic materials, Adv. Colloid Interf. Sci. 70 (1997) 125-169.
- [6] M. Capece, J. Barrows, R.N. Davé, RESEARCH ARTICLE: controlled release from drug microparticles via solventless dry-polymer coating, J. Pharm. Sci. 104 (2015)
- [7] M. Capece, R.N. Davé, Solventless polymer coating of microparticles, Powder Technol. 261 (2014) 118-132.
- [8] M. Capece, Z. Huang, To, D, M. Aloia, C. Muchira, R.N. Davé, A.B. Yu, Prediction of porosity from particle scale interactions; surface modification of fine cohesive powders, Powder Technol. 254 (2014) 103-113.
- A. Castellanos, The relationship between attractive interparticle forces and bulk behaviour in dry and uncharged fine powders, Adv. Phys. 54 (2005) 263–276.

  [10] L. Chen, X. Ding, Z. He, Z. Huang, K.T. Kunnath, K. Zheng, R.N. Davé, Surface
- engineered excipients: I. improved functional properties of fine grade microcrystalline cellulose, Int. J. Pharm. 536 (2018) 127–137.
- [11] W. Chen, R.N. Dave, R. Pfeffer, O. Walton, Numerical simulation of Mechanofusion system, Powder Technol, 146 (2004) 121-136.
- [12] Y. Chen, J. Yang, R.N. Dave, R. Pfeffer, Fluidization of coated group C powders, AICHE I. 54 (2008) 104–121.
- [13] Y. Chen, J. Yang, A. Mujumdar, R. Dave, Fluidized bed film coating of cohesive Geldart group C powders, Powder Technol. 189 (2009) 466-480.
- [14] R. Dave, W. Chen, A. Mujumdar, W. Wang, R. Pfeffer, Numerical simulation of dry particle coating processes by the discrete element method, Adv. Powder Technol. 14 (2003) 449–470.

- [15] X. Deng, I. Scicolone, X. Han, R.N. Davé, Discrete element method simulation of a conical screen mill: a continuous dry coating device. Chem. Eng. Sci. 125 (2015)
- [16] X. Deng, K. Zheng, R.N. Davé, Discrete element method based analysis of mixing and collision dynamics in adhesive mixing process, Chem. Eng. Sci. 190 (2018) 220-231.
- [17] S.S. Dukhin, J. Yang, R.N. Dave, R. Pfeffer, Deactivated sintering by particle coating: the significance of static and dynamic surface phenomena, Colloids Surf. A Physicochem. Eng. Asp. 235 (2004) 83-99.
- [18] C. Ghoroi, L. Gurumurthy, D.J. McDaniel, L.J. Jallo, R.N. Davé, Multi-faceted characterization of pharmaceutical powders to discern the influence of surface modification, Powder Technol. 236 (2013) 63-74.
- C. Ghoroi, X. Han, To, D. L. Jallo, L. Gurumurthy, R.N. Davé, Dispersion of fine and ultrafine powders through surface modification and rapid expansion, Chem. Eng. Sci. 85 (2013) 11-24.
- X. Han, C. Ghoroi, R. Davé, Dry coating of micronized API powders for improved dissolution of directly compacted tablets with high drug loading, Int. J. Pharm. 442 (2013) 74-85
- [21] X. Han, C. Ghoroi, To, D, Y. Chen, R. Davé, Simultaneous micronization and surface modification for improvement of flow and dissolution of drug particles, Int. J. Pharm. 415 (2011) 185-195.
- [22] X. Han, L. Jallo, D. To, C. Ghoroi, R. Davé, Pharmaceutics, drug delivery and pharmaceutical technology: passivation of high-surface-energy sites of milled ibuprofen crystals via dry coating for reduced cohesion and improved flowability, J. Pharm. Sci. 102 (2013) 2282-2296.
- [23] J.A. Hersey, Ordered mixing: a new concept in powder mixing practice, Powder Technol. 11 (1975) 41-44.
- H. Honda, M. Kimura, F. Honda, T. Matsuno, M. Koishi, Preparation of monolayer particle coated powder by the dry impact blending process utilizing mechanochemical treatment, Colloids Surf. A Physicochem. Eng. Asp. 82 (1994) 117-128.
- Z. Huang, J.V. Scicolone, L. Gurumuthy, R.N. Davé, Flow and bulk density enhancements of pharmaceutical powders using a conical screen mill: a continuous dry coating device, Chem. Eng. Sci. 125 (2015) 209-224.
- Z. Huang, J.V. Scicolone, X. Han, R.N. Davé, Improved blend and tablet properties of fine pharmaceutical powders via dry particle coating, Int. J. Pharm. 478 (2015) 447-455
- [27] Z. Huang, W. Xiong, K. Kunnath, S. Bhaumik, R.N. Davé, Improving blend content uniformity via dry particle coating of micronized drug powders, Eur. J. Pharm. Sci. 104 (2017) 344-355.
- S. Inaba, S. Todaka, Y. Ohta, K. Morinaga, Equation for estimating the Young's Modulus, Shear Modulus and Vickers hardness of aluminosilicate glasses, J. Jpn. Inst. Metals 64 (2000) 177-183.
- [29] J.N. Israelachvili, Intermolecular and surface forces, Burlington: Elsevier Science 2011 (2011) 3.
- L.J. Jallo, C. Ghoroi, L. Gurumurthy, U. Patel, R.N. Davé, Improvement of flow and bulk density of pharmaceutical powders using surface modification, Int. J. Pharm. 423 (2012) 213-225.
- L.J. Jallo, M. Schoenitz, E.L. Dreizin, R.N. Dave, C.E. Johnson, The effect of surface modification of aluminum powder on its flowability, combustion and reactivity, Powder Technol. 204 (2010) 63-70.
- [32] K.L. Johnson, Contact Mechanics, Cambridge University Press, Cambridge [Cambridgeshire]; New York, 1987 1987.
- [33] S. Jonat, S. Hasenzahl, M. Drechsler, P. Albers, K.G. Wagner, P.C. Schmidt, Investigation of compacted hydrophilic and hydrophobic colloidal silicon dioxides as glidants for pharmaceutical excipients, Powder Technol. 141 (2004) 31-43.
- K. Kunnath, Z. Huang, L. Chen, K. Zheng, R. Davé, Improved properties of fine active pharmaceutical ingredient powder blends and tablets at high drug loading via dry particle coating, Int. J. Pharm. 543 (2018) 288–299.
- [35] Q. Li, V. Rudolph, W. Peukert, London-van der Waals adhesiveness of rough particles, Powder Technol. 161 (2006) 248-255.
- A. Mujumdar, D. Wei, R.N. Dave, R. Pfeffer, C.-Y. Wu, Improvement of humidity resistance of magnesium powder using dry particle coating, Powder Technol. 140 (2004)
- [37] M. Mullarney, L. Beach, B.A. Langdon, M. Polizzi, Applying dry powder coatings: using a resonant acoustic mixer to improve powder flow and bulk density, Pharm. Technol. 35 (2011) 94-102.
- [38] M.P. Mullarney, L.E. Beach, R.N. Davé, B.A. Langdon, M. Polizzi, D.O. Blackwood, Applying dry powder coatings to pharmaceutical powders using a comil for improving powder flow and bulk density, Powder Technol. 212 (2011) 397–402.
- M. Naito, H. Abe, K. Sato, Nanoparticle bonding technology for the structural control of particles and materials, J. Soc. Powder Technol. Jpn 42 (2005) 625-631.
- M. Naito, A. Kondo, T. Yokoyama, Applications of comminution techniques for the surface modification of powder materials, ISII Int. 33 (1993) 915-924.
- [41] D. Nguyen, A. Rasmuson, I. Niklasson Björn, K. Thalberg, Mechanistic time scales in adhesive mixing investigated by dry particle sizing, Eur. J. Pharm. Sci. 69 (2015) 19-25.
- J.G. Osorio, F.J. Muzzio, Evaluation of resonant acoustic mixing performance, Powder Technol, 278 (2015) 46-56.
- [43] D. Paiva, A.M. Pereira, A.L. Pires, J. Martins, L.H. Carvalho, F.D. Magalhães, Reinforcement of thermoplastic corn starch with crosslinked starch/chitosan microparticles, Polymers (2018) 10.
- [44] R. Patel, J. Liu, J. Scicolone, S. Roy, S. Mitra, N. Dave, Z. Iqbal, Formation of stainless steel-carbon nanotube composites using a scalable chemical vapor infiltration process, J. Mater. Sci. 48 (2013) 1387-1395.
- P. Patrício, The hertz contact in chain elastic collisions, Am. J. Phys. 72 (2004) 1488-1491.

- [46] E. Peçanha, M. Albuquerque, R. Simão, L. Leal Filho, M. Monte, Interaction forces between colloidal starch and quartz and hematite particles in mineral flotation, Colloids Surf. A Physicochem. Eng. Asp. 562 (2018).
- [47] R. Pfeffer, R.N. Dave, D. Wei, M. Ramlakhan, Synthesis of engineered particulates with tailored properties using dry particle coating, Powder Technol. 117 (2001) 40–67.
  [48] M. Ramlakhan, C.Y. Wu, S. Watano, R.N. Dave, R. Pfeffer, Dry particle coating using
- [48] M. Ramlakhan, C.Y. Wu, S. Watano, R.N. Dave, R. Pfeffer, Dry particle coating using magnetically assisted impaction coating: modification of surface properties and optimization of system and operating parameters, Powder Technol. 112 (2000) 137–148.
   [49] M. Ramlakhan Mohan, N. Dave, R. Pfeffer, Promotion of deactivated sintering by dry-
- [49] M. Ramlakhan Mohan, N. Dave, R. Pfeffer, Promotion of deactivated sintering by dryparticle coating, AICHE J. 49 (2003) 604–618.
- [50] P. Singh, T.K.S. Solanky, R. Mudryy, R. Pfeffer, R. Dave, Estimation of coating time in the magnetically assisted impaction coating process, Powder Technol. 121 (2001) 159–167.
- [51] C. Thornton, Z. Ning, A theoretical model for the stick/bounce behaviour of adhesive, elastic- plastic spheres, Powder Technol. 99 (1998) 154–162.
- K. Wang, M.W. Chen, D. Pan, T. Fujita, W. Zhang, X.M. Wang, A. Inoue, Plastic deformation energy of bulk metallic glasses, Mater. Sci. Eng. B 148 (2008) 101–104.
- [53] J. Yang, A. Sliva, A. Banerjee, R.N. Dave, R. Pfeffer, Dry particle coating for improving the flowability of cohesive powders, Powder Technol. 158 (2005) 21–33.
  [54] T. Yokoyama, K. Urayama, M. Naito, M. Kato, T. Yokoyama, The angmill
- 54] T. Yokoyama, K. Urayama, M. Naito, M. Kato, T. Yokoyama, The angmill mechanofusion system and its applications, KONA Powder Part. J. 5 (1987) 59–68.
- [55] Q. Zhang, J. Yang, S. Teng, R.N. Dave, L. Zhu, P. Wang, M.-W. Young, C.G. Gogos, Insitu, simultaneous milling and coating of particulates with nanoparticles, Powder Technol. 196 (2009) 292–297.